JOC*Article*

Bis(phosphine Imide)s: Easily Tunable Organic Electron Donors

Vanina V. Guidi, Zhou Jin, Devin Busse, William B. Euler, and Brett L. Lucht*

Department of Chemistry, University of Rhode Island, Kingston, Rhode Island 02881

blucht@chm.uri.edu

Received June 13, 2005

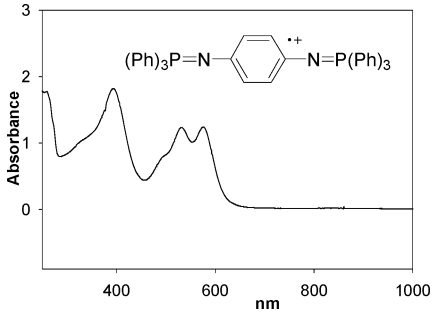

The electrochemical, structural, and spectroscopic properties of bis(phosphine imide)s have been investigated. *p*-Phenylenebis(phosphine imide)s $Ar_3PNC_6H_4NPAr_3$ (**1a**−**d**) have two reversible single-electron oxidations. The first oxidation potentials can be varied from −0.05 to 0.15 V (versus SCE) by modification of the substituents on phosphorus (Ar). Electron-donating substituents lower the oxidation potential, while electron-withdrawing substituents increase the oxidation potential. The difference between the first and second oxidation potential (ΔE, 0.41−0.50) and the electronic coupling (H_{ab}, 1.1 eV) are similar for **1a**−**d**. Computational (DFT) and UV−visible−NIR spectroscopic investigations of **1a**−**d** suggest that the first oxidation leads to a delocalized radical cation $\mathbf{1a}^{\bullet+}$ while the second oxidation leads to a quinonoidal dicationic state $\mathbf{1a}^{2+}$. The aromatic linker between phosphine imides has also been modified. Upon oxidation, *N*,*N*′-4,4′-biphenylene(bis(triphenyl)-phosphine imide) (**3**) forms radical cationic and a dicationic species similar to **1a**−**d**. While ΔE (0.18 V) and H_{ab} (0.63 eV) are smaller, suggesting weaker electronic communication between the two P═N units in the radical cationic state, the presence of NIR absorptions with vibrational fine structure (768, 861, and 983 nm) supports the formation of delocalized radical cation for $\mathbf{3}^{\bullet+}$.

Introduction

One of the important uses for conjugated organic materials is the preparation of organic light emitting diodes (OLEDs) and polymer light emitting diodes (PLEDs).[1] The initial investigations of PLEDs were simple single-layer devices where the conjugated polymer, typically poly(*p*-phenylene vinylene), was placed between a positive and a negative electrode.[2] As the field of OLEDs and PLEDs developed, the preferred architecture evolved into a three-layer device consisting of a hole transport layer, light emitting layer, and an electron transport layer. The addition of the hole transport and electron transport layers allows easier hole and electron injection into the emissive layer, which provides devices that operate at significantly lower voltages and have longer lifetimes.[3] The reversible generation of radical cations is required for good organic hole transporting materials. The most widely used hole transport materials include triarylamines such as 4,4′-bis-(*m*-tolylphenylamino)biphenyl (TPD) and poly(*N*-vinylcarbazole) (PVK) (Chart 1).[4] While many polymer or conjugated organic materials have been used as electron transport layers, the number of good hole transport materials is limited. Thus, the investigation of novel organic materials that

(1) (a) *Handbook of Conducting Polymers*; Skotheim, T. A., Ed.; Marcel Dekker: New York, 1986. (b) Fichou, D. In *Conjugated Polymers: The Novel Science and Technology of Highly Conducting and Nonlinear Optically Active Materials*; Bredas, J. L., Silbey, R., Eds.; Kluwer Academic: Dordecht, The Netherlands, 1991.

(2) Burroughs, J. H.; Bradley, D. D. C.; Brown, A. R.; Marks, R. N.; Mackay, K.; Friend, R. H.; Burns, P. L.; Holmes, A. B. *Nature* **1990**, *347*, 539.

(3) Kraft, A.; Grimsdale, A. C.; Holmes, A. B. *Angew. Chem., Int. Ed.* **1998**, *37*, 402.

(4) Anderson, J. D.; McDonald, E. M.; Lee, P. A.; Anderson, M. L.; Ritchie, E. L.; Hall, H. K.; Hopkins, T.; Mash, E. A.; Wang, J.; Padias, A.; Thayumanavan, S.; Barlow, S.; Marder, S. R.; Jabbour, G. E.; Shaheen, S.; Kippelen, B.; Peyghambarian, N.; Wightman, R. M.; Armstrong, N. R. *J. Am. Chem. Soc.* **1998**, *120*, 9646.

10.1021/jo051196u CCC: $30.25 © 2005 American Chemical Society
Published on Web 08/20/2005

CHART 1

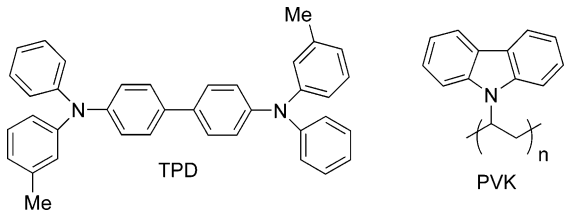

form stable radical cations is important for improvements in OLEDs and PLEDs. Although many of the conjugated polymers and related conjugated organic materials have utilized both sulfur and nitrogen,[1,4,5] the investigation of the electronic properties of phosphorus containing organic materials has only recently received significant attention.[6−9]

Phosphine imides are related to the widely investigated phosphazenes. Phosphazenes have four σ-bonds to phosphorus and thus no available p-orbital for involvement in π-conjugation. However, the bond angles and lengths support delocalization limited to P−N−P units.[10] The nature of the phosphorus−nitrogen double bond is debatable, but recent results argue against significant involvement of the d-orbitals on phosphorus and support a combination of σ-bonding and some degree of π-back-bonding from N into the σ^* orbitals of P.[11] Infrared spectroscopic investigations of the P═N bond stretch of *p*-substituted phenylphosphine imides support an expansion of conjugation due to the electron-donating effect of the phosphine imide and increasing quinonoidal character of the aromatic ring (eq 1).[12]

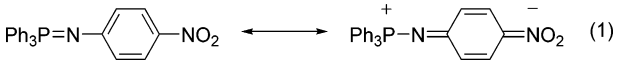

The electrochemical and spectroscopic investigation of *N*,*N*′-*p*-phenylene(bis(triphenyl)phosphine imide) ($Ph_3P{=}NC_6H_4N{=}PPh_3$, **1a**) has been recently reported.[13] Phosphine imides are prepared in high yields via the Staudinger reaction of aryl azides with triaryl phosphines.[14] Investigation of the electronic properties of phosphine imide-based materials suggests that *p*-phenylenebis(phosphine imide)s are good organic electron donors. **1a** is stable to atmospheric conditions and has two reversible single-electron oxidations (0.043 and 0.547 V versus saturated calomel electrode (SCE)). This supports the formation of stable radical cationic and dicationic species. Results of spectroscopic and electrochemical investigations of poly(*p*-phenylene phosphine imide)s (**2**) are similar to **1a**, suggesting formation of localized radical cations on the polymer chains and electronically insulating phosphorus atoms. The formation of stable radical cationic species at potentials comparable to tetrathiafulvalene (TTF) indicates that bis(phosphine imide)s are good electron donors and may be useful as hole transport materials.

TABLE 1. Oxidation Potentials of Bis(phosphine Imide)s[a]

compound	E_1	E_2	$\Delta E = (E_1 - E_2)$
1a	0.04	0.55	0.50
1b	−0.05	0.40	0.45
1c	−0.02	0.47	0.49
1d	0.15	0.56	0.41
3	0.36	0.54	0.18

[a] 1 mM solution in 0.1 M TBATFB in CH_2Cl_2. $E_{1,2}$: Electrode potentials (volts) referenced to SCE. E_1: Potential of radical cation. E_2: Potential of dication.

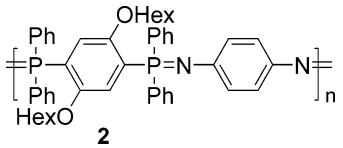

2

This report is an expansion of our initial studies of the electronic properties of **1a** and the related polymers (**2**). We have investigated a variety of bis(phosphine imide)s via modification of both the substitutents on phosphorus and the aromatic linking unit between bis(phosphine imide)s. The properties of the bis(phosphine imide)s have been characterized by a combination of cyclic voltammetry (CV), absorption spectroscopy (UV−vis−NIR), single-crystal X-ray diffraction, and density functional theory (DFT) calculations.

Results

Bis(phosphine imide)s **1a**−**d**[15,16] and **3**[17] were prepared, purified, and identified following literature procedures.

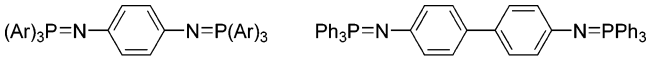

Ar = C_6H_5, **1a**; *p*-$C_6H_4OCH_3$, **1b**; *p*-$C_6H_4CH_3$, **1c**; *p*-C_6H_4F, **1d**.

3

Cyclic Voltammetry. Investigation of substituted bis(phosphine imide)s suggests that the electron-donating substituents can stabilize the positive charge on phosphorus and improve the electron-donating ability while electron-withdrawing substituents reduce the donor properties (Table 1, Figure 1). The electron-donating *p*-methoxyphenyl substituents of **1b** significantly lower the oxidation potentials of the bis(phosphine imide). Two single-electron oxidations are observed at −0.05 and 0.40 V versus SCE (oxidation potentials for **1a** are 0.04 and

(5) Ferraro, J. R.; Williams, J. M. *Introduction to Synthetic Electrical Conductors*; Academic Press: Orlando, FL, 1987.
(6) Cosmina, D.; Shashin, S.; Smith, R. C.; Choua, S.; Berclaz, T.; Geoffroy, M.; Protasiewicz, J. D. *Inorg. Chem.* **2003**, *42*, 6241.
(7) (a) Bevierre, M. O.; Mercier, F.; Ricard, L.; Mathey, F. *Angew. Chem., Int. Ed. Engl*. **1990**, *29*, 655. (b) Deschamps, E.; Ricard, L.; Mathey, F. *Angew. Chem., Int. Ed. Engl*. **1994**, *33*, 1158.
(8) (a) Lucht, B. L.; St. Onge, N. O. *Chem. Commun*. **2000**, 2097. (b) Jin, Z.; Lucht, B. L. *J. Organomet. Chem.* **2002**, *653*, 167. (c) Jin, Z.; Lucht, B. L. *J. Am. Chem. Soc.* **2005**, *127*, 5586.
(9) (a) Wright, V. A.; Gates, D. P. *Angew. Chem., Int. Ed*. **2002**, *41*, 2389. (b) Smith, R. C.; Chen, X.; Protasiewicz, J. D. *Inorg. Chem.* **2003**, *42*, 5468.
(10) (a) Blonsky, P. M.; Shriver, D. F.; Austin, P.; Allcock, H. R. *J. Am. Chem. Soc.* **1984**, *106*, 6854. (b) Gray, F. M. *Solid Polymer Electrolytes: Fundamentals and Technological Applications*; VCH: New York, 1991. (c) Neilson, R. H. Phosphorus−Nitrogen Compounds. In *Encyclopedia of Inorganic Chemistry*; King, B. R., Ed.; Wiley & Sons: New York, 1994; Vol. 6, pp 3180−3199.
(11) Sudhakar, P. V.; Lammertsma, K. *J. Am. Chem. Soc*. **1991**, *113*, 1899.
(12) Wiegrabe, W.; Bock, H. *Chem. Ber*. **1968**, *101*, 1414.
(13) Escobar, M.; Jin, Z.; Lucht, B. L. *Org. Lett*. **2002**, 2213.
(14) Abel, E. W.; Mucklejohn, S. A. *Phosphorus Sulfur* **1981**, *9*, 235.
(15) Herring, D. L. *J. Org. Chem.* **1961**, *26*, 3998.
(16) Khmurova, I. N.; Yurchenko, V. G.; Kukhar, V. P.; Zolotareva, L. A. *Zh. Obshch. Khim.* **1974**, *44*, 74.
(17) Homer, L.; Oediger, H. *Ann.* **1959**, *627*, 142.

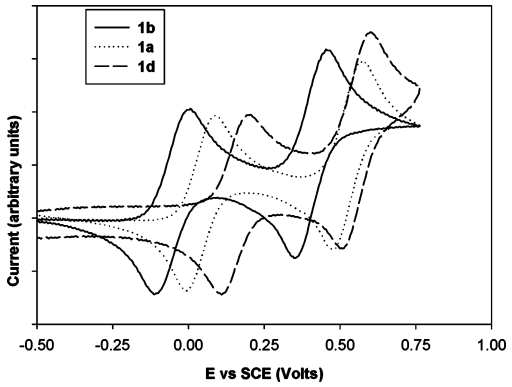

FIGURE 1. Cyclic voltammograms for compounds **1a**, **1b**, and **1d**.

SCHEME 1

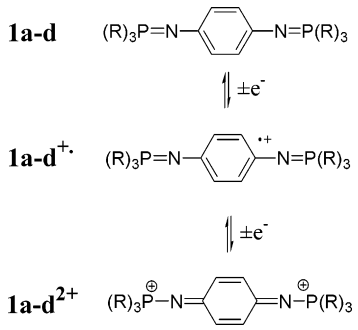

0.55 V versus SCE). Alternatively, the electron-withdrawing *p*-fluorophenyl substituents of **1d** increase the oxidation potential (0.15 and 0.56 V versus SCE). As expected, **1c** has an oxidation potential lower than that of **1a** due to the superior electron-donating properties of an alkyl group versus hydrogen. The results suggest that the oxidation potentials of bis(phosphine imide)s can be easily tuned via modification of the substituents on phosphorus. The oxidation potentials of **1a**−**d** are comparable to the most widely investigated organic electron donors, such as TTF.[18] However, TTF derivatives require much more complicated syntheses, making chemical modification of the oxidation potentials difficult.[19]

Both the radical cation and dications of **1a**−**d** are stable. Chloroform solutions of $\mathbf{1a}^{\bullet+}$ can be stored at room temperature in the presence of atmospheric oxygen and moisture for weeks with no apparent degradation. The structure of the oxidized bis(phoshine imide) **1a** has been investigated by DFT, as discussed later in the article, and is consistent with the stepwise formation of a radical cation and dication as depicted in Scheme 1. The quinonediimine structure of $\mathbf{1a}^{2+}$ is consistent with the observed stability and low oxidation potential for formation.

In all cases, the two single-electron oxidations of **1a**−**d** appear reversible. The reversibility of the oxidations was confirmed for **1b** by monitoring the intensity of the anodic peaks at different scan rates. A linear plot of I_p versus the square root of the scan rate was observed, confirming the reversibility of the redox process.[20]

TABLE 2. UV−Visible−NIR Data of Bis(phosphine Imide)s[a]

compound	neutral λ_{max} nm ($\epsilon_{max} \times 10^{-3}$)	radical cation $X^{\bullet+}$ λ_{max} nm ($\epsilon_{max} \times 10^{-3}$)
1a	263 (17), 319 (sh)	394 (46), 492 (sh), 531 (31), 576 (31)
1b	317 (sh)	395 (30), 539 (22), 491 (sh), 580 (22)
1c	262 (sh), 318 (sh)	396 (42), 496 (sh), 530 (28), 577 (30)
1d	262 (sh), 319 (sh)	392 (34), 491 (sh), 533 (22), 576 (24)
3	318 (14)	458 (sh), 499 (12), 768 (sh), 861 (8), 983 (17)

[a] UV−visible spectra were recorded in either $CHCl_3$ or CH_2Cl_2. Both solvents gave similar spectra. The wavelength maximum and absorption coefficient ($\epsilon_{max} \times 10^{-3}$) are provided for each major absorption. (sh) Indicates absorption is a shoulder.

The difference between the first and second oxidation potential (ΔE) for **1a**−**d** is between 0.41 and 0.50 V. While ΔE has been used as measure of the degree of electronic communication, it can be misleading.[21] However, the similarity of ΔE values for **1a**−**d** suggests comparable delocalization of radical cations $\mathbf{1a}^{\bullet+}$−$\mathbf{d}^{\bullet+}$. The ΔE values of **1a**−**d** are similar to those reported for *N*,*N*,*N*′,*N*′-tetra(4-methoxyphenyl)-1,4,-phenylenediamine, 0.49 V,[22] and *N*,*N*,*N*′,*N*′-tetramethylphenylenediamine (TMPD), 0.57 V,[23] and support strong electronic coupling between P═N units via the phenylene linker consistent with a delocalized radical cation.

In addition to modification of the substituents on phosphorus, the aromatic linker between phosphine imides can be easily modified. The investigation of **3**, which has been prepared from benzidene and triphenylphosphine, is particularly interesting since **3** has the same bridging group as TPD. Cyclic voltammetry of **3** provides results similar to those observed for **1a**−**d**. Two reversible single-electron oxidations are observed for **3**. The higher first oxidation potential (0.36 versus SCE) and smaller ΔE of **3** (0.18 versus 0.45 V for **1a**) suggest weaker electronic coupling between phosphine imides.[22]

UV−Visible−NIR Absorption Spectroscopy. The absorption spectra of **1a**−**d** were investigated in the neutral, cationic, and dicationic states. The absorption maxima are summarized in Table 2. The absorption spectra for neutral compounds **1a**−**d** are similar, with two high-energy absorption maxima characteristic of the localized aromatic rings on phosphorus and in the linking phenylenediamine (λ_{max} = 260−265 nm, 345−355 nm).

Chemical oxidation of the bis(phosphine imide)s was conducted under an inert atmosphere and followed by UV−visible−NIR absorption spectroscopy. Representative spectra of the chemical oxidation of **1a** are shown in Figure 2. Upon oxidation to the radical cation, several new absorption bands are observed for **1a**−**d** at longer wavelength (350−600 nm). The new low energy bands result from absorptions of the radical cation and are similar to those observed for TMPD[24,25] and bis(3-oxo-9-

(18) Torrance, J. B. *Mol. Cryst. Liq. Cryst.* **1985**, *126*, 55.
(19) Roncali, J. *J. Mater. Chem.* **1997**, *12*, 2307.
(20) *Laboratory Techniques in Electroanalytical Chemistry*; Kissinger, P. T., Heineman, W. R., Eds.; Marcel Dekker: New York, 1985.
(21) Barriere, F.; Camire, N.; Geiger, W. E.; Mueller-Westerhoff, U. T.; Sanders, R. *J. Am. Chem. Soc.* **2002**, *124*, 7262.
(22) Lambert, C.; Noll, G. *J. Am. Chem. Soc.* **1999**, *121*, 8434.
(23) Nelsen, S. F.; Kessel, C. R.; Brien, D. J. *J. Am. Chem. Soc.* **1980**, *102*, 702.
(24) Shida, T. *Electronic Absorption Spectra of Radical Ions*; Elsevier: Amsterdam, 1988.

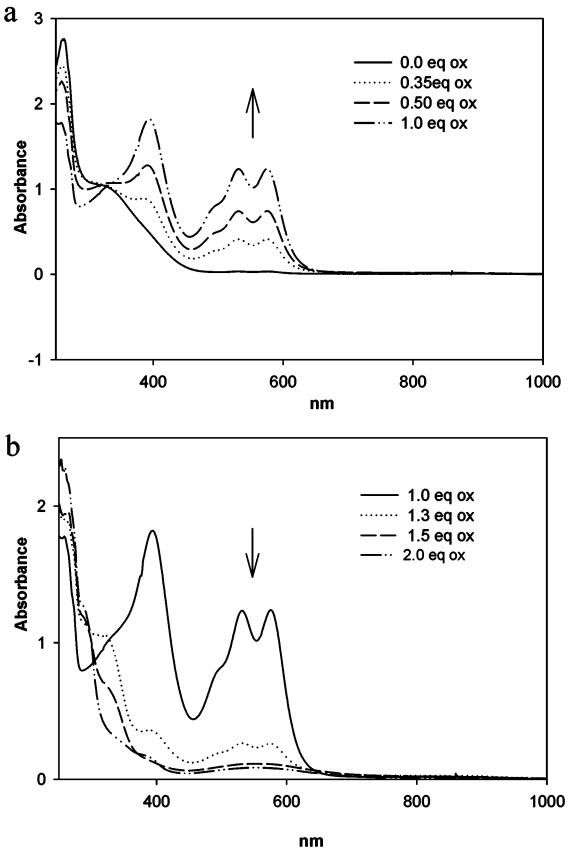

FIGURE 2. UV−visible−NIR spectra of the stepwise oxidation of **1a** (40 μM in $CHCl_3$) to **1a**$^{\bullet+}$ (a) and **1a**$^{2+}$ (b).

azabicyclo[3.3.1]non-9-yl)benzene).[25,26] Further oxidation to the dication results in a loss of the low energy absorptions characteristic of the radical cation. The dications have short wavelength <300 nm absorption maxima, but the absorptions are difficult to quantitatively characterize due to overlapping absorptions of the chemical oxidant, bistrifluoroacetoxyiodobenzene, utilized in these investigations.

Chemical oxidation of **3** provided similar results (Figure 3). Upon removal of a single electron to generate **3**$^{\bullet+}$, several new absorptions were observed. In addition to the longer wavelength absorption bands in the visible spectrum (458 and 499 nm), three new absorption bands are observed in the NIR (768, 861, and 983 nm). The new low energy absorptions are similar to those observed in *N*,*N*,*N*′,*N*′-tetramethylbenzidene (TMB).[24] The presence of vibrational fine structure is characteristic of delocalized radical cations.[27] The steric interactions present in the biphenyl unit result in a decrease in the electronic coupling between P═N units as evidenced by the lower energy absorptions. Changing the solvent from CH_2Cl_2 to acetonitrile did not result in a significant change in the NIR absorption bands (768, 859, and 978), consistent with delocalized species.[28] The addition of a second

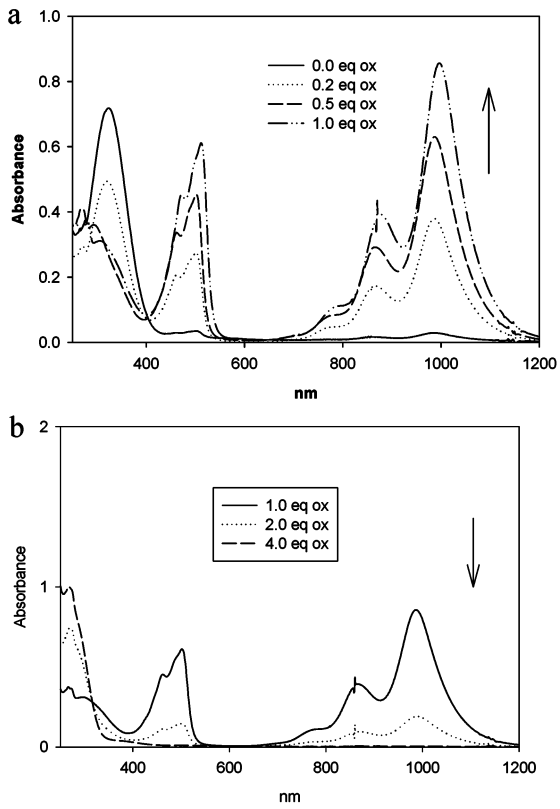

FIGURE 3. UV−visible−NIR spectra of the stepwise oxidation of **3** (50 μM in $CHCl_3$) to **3**$^{\bullet+}$ (a) and **3**$^{\bullet+}$ to **3**$^{2+}$ (b).

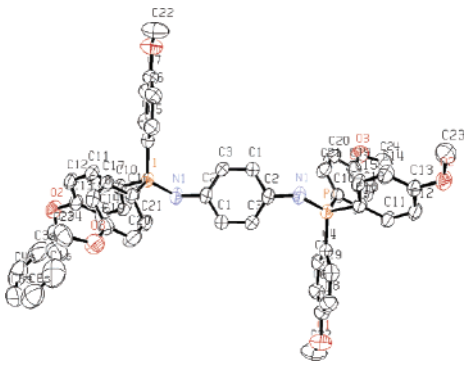

FIGURE 4. X-ray structure of **1b**.

equivalent of oxidant to **3**$^{\bullet+}$ to generate the dication results in the loss of low energy absorption bands, consistent with the formation of a dication.

Single-Crystal X-ray Diffraction. Suitable crystals of **1b** were prepared via crystallization from benzene and analyzed by single-crystal X-ray diffraction (Figure 4). The structure of **1b** has an inversion center in the middle of the central aromatic ring and P═N bonds (156.2(2) pm) comparable to those previously reported for *N*-*p*-bromophenyl triphenylphosphine imide (**4**, 156.7 pm).[29] The C−P bond lengths are not equivalent. Two short bonds (P(1)−C(10) 179.9(2) and P(1)−C(4) 180.6(2) pm) and one long bond (P(1)−C(16) 181.6(2) pm) are observed. In addition, the C(4)−P(1)−C(10) bond angle is large, 106.2-(10)°, while the C(4)−P(1)−C(16) and C(10)−P(1)−C(16)

(25) Bailey, S. E.; Zink, J. I.; Nelsen, S. F. *J. Am. Chem. Soc.* **2003**, *125*, 5939.
(26) Nelsen, S. F.; Weaver, M. N.; Telo, J. P.; Lucht, B. L.; Barlow, S. *J. Org. Chem.* Submitted.
(27) Nelsen, S. F. *Chem.−Eur. J.* **2000**, *6*, 581.
(28) Brunschwig, B. S.; Creutz, C.; Sutin, N. *Chem. Soc. Rev.* **2002**, *31*, 168.

(29) Hewlins, M. J. E. *J. Chem. Soc. B* **1971**, 942.

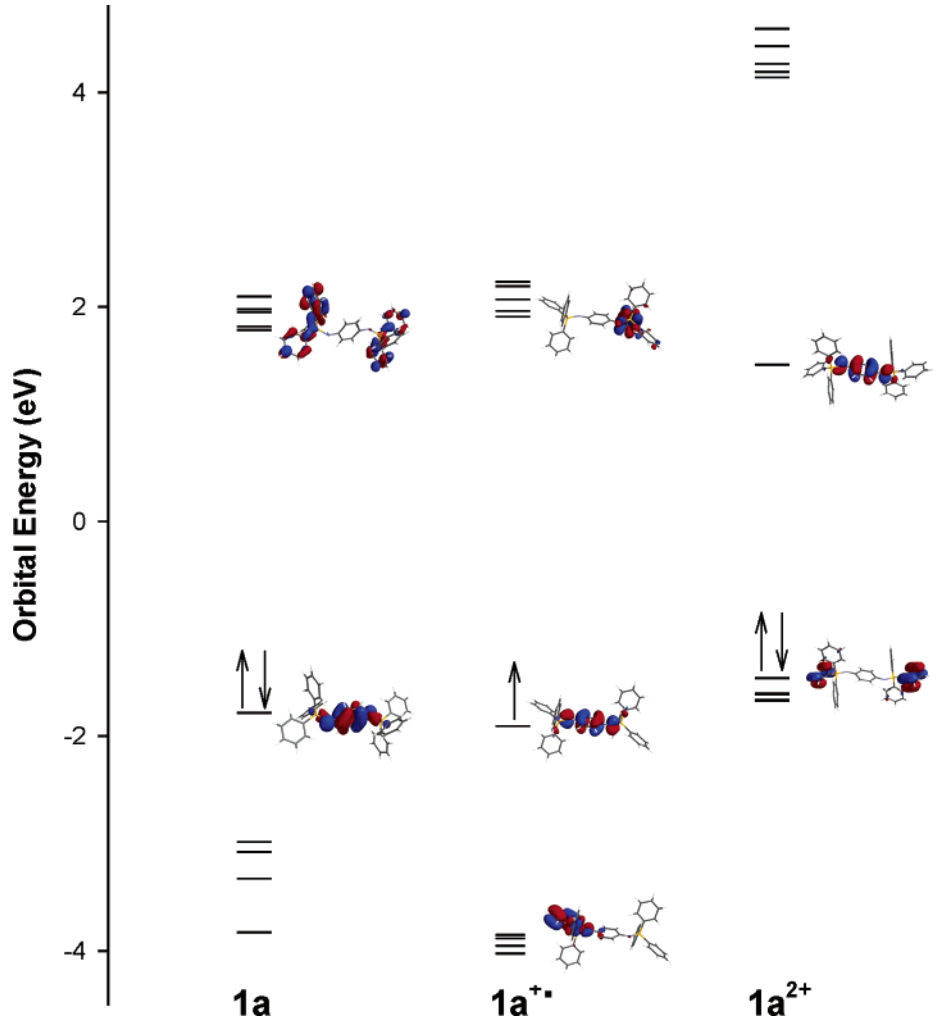

FIGURE 5. Orbital energy diagram for **1a**, **1a**$^{\bullet+}$, and **1a**$^{2+}$. The zero of energy was set to be mid gap in each case.

bond angles are small (104.2(10) and 104.8(10)°, respectively). Similar bond asymmetry is observed for C−P bonds in **4**.[29] The C−P−C bond angles and C−P bond lengths are consistent with π-back-bonding from N to P, which weakens and lengthens the P−C bond.[30] The asymmetry of P−C bond lengths suggests that the π-back-bonding from N is largely oriented into the σ^* orbital of the P(1)−C(16) bond. Interestingly, the P(1)−C(16) bond is nearly perpendicular to the P1−N1−C2 plane, consistent with this model.

Density Functional Theory Calculations. DFT calculations were conducted on bis(phosphine imide)s **1a**, **1a**$^{\bullet+}$, and **1a**$^{2+}$. The structures were optimized using the B3LYP functional and the 6-31G** basis set in the Spartan quantum chemical program suite.[31] The calculations strongly agree with many of the spectroscopically and crystallographically observed properties of **1a**−**d**. Neutral **1a** has localized P=N double bonds (155.1 pm), compared to 156.2 pm in the X-ray structure for **1b** (Figure 4), long C−N bonds (140.3 pm), and a large dihedral angle between the P=N bond and the central aromatic ring (~78°), indicating little conjugation between the P=N double bond and the benzene ring. Upon one-electron oxidation, the P−N bonds become longer (162.3 and 158.5 pm), the C−N bonds become shorter (131.5 and 134.4 pm), and the P−N−C plane and the central *p*-phenylenediamine ring become nearly coplanar (dihedral angles less than 5°), indicating the development of the quinonediimine structure. The charge and spin densities for **1a**$^{\bullet+}$ demonstrate that the oxidation has occurred primarily from the N lone pairs and the ipso C atom π-orbitals (~70% of the spin density and about 45% of the positive charge is located on these four atoms). In **1a**$^{\bullet+}$, the charge density of P is nearly the same as that in **1a** and there is no spin density found on the P atoms, indicating that the P atom is unaffected by the removal of the electron. Upon further oxidation to **1a**$^{2+}$, the quinonediimine structure fully develops. The C−N bonds are found to be 126.5 pm, clearly a double bond, while the P−N bond increases to 166.6 pm, close to a single bond length. Again, there is little increased charge density on the P atoms: the ionic charge resides on the N atoms and the central benzene ring. Finally, the calculated P−C bond angles and lengths for **1a** are similar to those of **1b**. Upon oxidation to **1a**$^{\bullet+}$ and **1a**$^{2+}$, the P−C bond inequivalency is lost and the P−C bond lengths are reduced, consistent with a loss of electronic donation into the σ^* orbitals of the P−C bonds.

(30) Dunne, B. J.; Morris, R. B.; Orpen, A. G. *J. Chem. Soc., Dalton Trans.* **1991**, 653.
(31) *Spartan* for Linux; Wavefunction, Inc.: Irvine, CA.

SCHEME 2

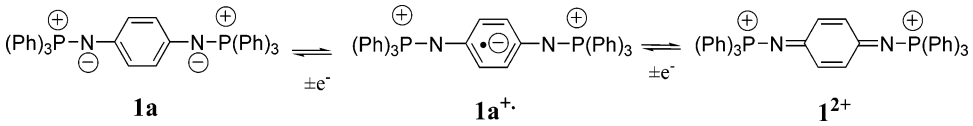

1a **1a**$^{+\cdot}$ **1**$^{2+}$

The orbital energy diagram for **1a**, **1a**$^{\bullet+}$, and **1a**$^{2+}$ is shown in Figure 5. In the reduced form, the highest occupied molecular orbital (HOMO) is a π-orbital located on the central ring and the N atoms while the lowest unoccupied molecular orbital (LUMO) is a π-orbital located on the peripheral phenyl groups. The HOMO−LUMO gap is calculated to be 3.6 eV. Upon one-electron oxidation to **1a**$^{\bullet+}$, the singly occupied molecular orbital (SOMO) is an N−ring−N π-orbital and is slightly lower in energy and the LUMO is slightly raised in energy so that the SOMO−LUMO gap is ~3.8 eV. In terms of the optical spectrum, however, the lowest energy excitation will be the HOMO to SOMO. These orbitals have a calculated energy difference of ~1.9 eV. Finally, in the dication the filled N−ring−N orbitals become much lower in energy so that in **1a**$^{2+}$ the HOMO is located on the peripheral phenyl rings and the LUMO is on the central ring and N atoms. The HOMO−LUMO gap in **1a**$^{2+}$ is found to be ~2.9 eV.

The computational results support little change of the charge on phosphorus upon oxidation. This suggests that the standard structure depicted for phosphine imides may be flawed. Recent investigations into the structure of phosphine oxides and phosphine imides support a highly polarized bond with significant π-back-bonding interaction between nitrogen and phosphorus. Our computational results support a highly polarized P−N bond with almost complete charge separation in **1a**. In fact, the stepwise oxidation of **1a** to **1a**$^{\bullet+}$ and **1a**$^{2+}$ might best be represented by Scheme 2. An electron-rich dianionic diamine is capped by cationic phosphonium ions. Electronic donation of the imine into the σ*-orbitals of the P−C bonds provides some additional stability to **1a**. The stepwise oxidation removes electrons from the central diamine unit with little change to the phosphonium ions.

Discussion

The tunability of the electron donor properties of **1a**−**d** is displayed in Table 1. Electron-donating substituents shift the oxidations to lower potential while electron-withdrawing substituents increase the oxidation potentials. The ready availability of many different phosphines allows straightforward synthetic modification of *p*-phenylenebis(phosphine imide)s and excellent control over the oxidation potential. The development of OLEDs requires hole injection materials with electronic structures that match the work function of the electrode materials allowing efficient hole transfer. Thus, *p*-phenylenebis(phosphine imide)s may make good hole transport materials for OLEDs.

Robin and Day developed a classification system of mixed valence compounds with three classes:[32] class I contains redox centers that are completely localized and behave separately, class II species have intermediate coupling between the two redox centers, and class III compounds are completely delocalized and have two equivalent redox centers with an intermediate oxidation state. Compounds **1a**$^{\bullet+}$−**d**$^{\bullet+}$ and **3**$^{\bullet+}$ have properties consistent with Robin and Day class III systems. The electronic coupling between redox sites for class III species can be measured from the energy of the optical transition using eq 2.[28]

$$h\nu_{max} = 2H_{ab} \quad (2)$$

H_{ab} = 1.08 and 0.63 eV for **1a**$^{\bullet+}$ and **3**$^{\bullet+}$, respectively. These values are similar to those determined for TMPD$^{\bullet+}$ and TMB$^{\bullet+}$, 1.01 and 0.61 eV, respectively.[33] **3** undergoes two reversible single-electron oxidations, but the first oxidation occurs at a higher potential and the ΔE is smaller (0.18 V) than that observed for **1a** (0.50 V). Changing the conjugated linker from phenyl in **1a** to biphenyl in **3** results in a decrease of ΔE and H_{ab}, suggesting weaker electronic coupling between P=N units via the biphenyl linker.

The combination of DFT calculations and single-crystal X-ray diffraction provides insight into the nature of the P=N bond in phosphine imides. The bond angles and lengths for the calculated structure of **1a** and the crystallographically determined structure of **1b** are similar. Upon oxidation, calculations indicate that the central aromatic ring shifts from a benzenoid structure in **1a** to a quinonoid structure in **1a**$^{2+}$ (Scheme 1). The change in structure of the central aromatic ring is accompanied by an 8% increase in the P−N bond length. However, there is little change in the charge on P going from **1a** to **1a**$^{\bullet+}$ and **1a**$^{2+}$. The increase of the P−N bond length is accompanied by a modest decrease in the P−C bond lengths (2−3%), consistent with a loss of electronic donation into the σ* orbitals on P. The results provide additional support for the recently proposed model for P=C, P=N, and P=O bonds, π-back-bonding from N into the σ* orbitals on P.[34]

Conclusions

The electrochemical, structural, and spectroscopic properties of aromatic bis(phosphine imide)s have been investigated. Aromatic bis(phosphine imide)s have two reversible one-electron oxidations at low potentials. The oxidation potentials of these novel organic electron donors can be easily modified via substituents on phosphorus. Electron-donating substituents lower the oxidation potential while electron-withdrawing substituents increase the oxidation potential. The aromatic linker between bis(phosphine imide) units can also be varied, allowing control over the electronic coupling between P=N units.

Experimental Procedures

Bis(phosphine imide)s **1a**−**d**[15,16] and **3**[17] were prepared, purified, and identified following literature procedures. A summary of the ^{1}H, ^{13}C NMR, and IR spectroscopic data for

(32) Robin, M.; Day, P. *Adv. Inorg. Chem. Radiochem*. **1967**, *10*, 247.

(33) Nelsen, S. F.; Tran, H. Q.; Nagy, M. A. *J. Am. Chem. Soc.* **1998**, *120*, 298.

(34) Gilheany, D. G. *Chem. Rev*. **1994**, *94*, 1339.

1b−**d** and **3** and a description for the general synthetic procedure for **1a**−**d** are included in the Supporting Information. Phosphines were purchased from a commercial supplier.

CV was performed on a Perkin-Elmer EG&G instruments Potentiostat and Galvanostat model 263A from Princeton Applied Research products, using the model K0264 micro-cell kit, K0265 silver/silver chloride reference electrode, K0266 counter electrode assembly (platinum 0.3-mm diameter counter electrode wire), and G0225 platinum microelectrode (working electrode). The scan rate was set at 50 mV/s. Two cycles were conducted for each system. No calibrations were made to compensate IR drops. A solution (1 mM) of compounds **1a**−**d** and **3** was prepared in a 0.1 M solution of tetrabutylammoniumtetrafluoroborate (TBATFB, 99%) in anhydrous CH_2Cl_2. TBATFB and CH_2Cl_2 were purchased from Aldrich and used as received. Electrode potentials were referenced to SCE by use of TTF (1 mM solution in the same electrolyte) as an external standard (0.30 and 0.66 V versus SCE).[35] The values of electrode potentials reported in Table 1 (E_1 and E_2) correspond to the average between the cathodic electrode potential (E_c) and the anodic electrode potential (E_a), $E_i = [E_a + E_c]/2$. ΔE corresponds to the gap between the electrode potentials as reported in Table 1, $\Delta E = [E_1 - E_2]$.

UV−vis−NIR spectra were acquired using a Perkin-Elmer Lambda 900 UV−visible−NIR spectrometer. Spectra of **1a**−**d** and **3** were taken for the neutral compound, radical cation, and dication. Chemical oxidation using bistrifluoroacetoxyiodobenzene ($PhI(OTF)_2$) was performed for each compound. All the solutions were prepared under N_2 using anhydrous solvents purchased from a commercial supplier and used as received.

Theoretical calculations were run using Spartan 02 (Build 114) for Linux 2.2.[31] No negative frequencies were found, indicating that the structures were minima. The electronic structures were calculated using DFT using the B3LYP hybrid functional and the 6-31G** basis set.

Crystals of compound **1b** for single-crystal X-ray diffraction were grown from anhydrous benzene at room temperature. The CIF is included in Supporting Information.

Acknowledgment. We thank the Donor of the Petroleum Research Fund for partial support of the work, A. Chandrasekaran and D. Venkaraman at the University of Massachusetts, Amherst, for acquisition of the X-ray structure of **1b**, and S. F. Nelsen, University of Wisconsin, Madison, for helpful discussions.

Supporting Information Available: Listings of the ^1H and ^{13}C NMR and IR absorptions for compounds **1b**−**d** and **3**, ^1H NMR spectra of **1b** and **1d**, ^{13}C spectrum for **1d**, CIF for **1b**, figure of molecular packing of **1b**, and complete details of the computational methods for **1a** including Cartesian coordinates and computed total energies. This material is available free of charge via the Internet at http://pubs.acs.org.

JO051196U

(35) Wheland, R. C.; Gillson, J. L. *J. Am. Chem. Soc.* **1976**, *98*, 3916.